RESEARCH ARTICLE

Pathological changes in the cerebellum of patients with multiple system atrophy and Parkinson's disease—a stereological study

Elisabeth H. L. Rusholt[1]; Lisette Salvesen[1]; Tomasz Brudek[1]; Betel Tesfay[1]; Bente Pakkenberg[1,2]; Mikkel V. Olesen[1] (iD)

[1] Research Laboratory for Stereology and Neuroscience, Department of Neurology, Bispebjerg-Frederiksberg Hospital, Nielsine Nielsens Vej 6B, DK-2400, Copenhagen, Denmark.
[2] Institute of Clinical Medicine, Faculty of Health and Medical Sciences, University of Copenhagen, Blegdamsvej 3, DK-2200, Copenhagen, Denmark.

Abstract

Multiple system atrophy (MSA) and Parkinson's disease (PD) are synucleinopathies characterized by aggregation of α-synuclein in brain cells. Recent studies have shown that morphological changes in terms of cerebral nerve cell loss and increase in glia cell numbers, the degree of brain atrophy and molecular and epidemiological findings are more severe in MSA than PD. In the present study, we performed a stereological comparison of cerebellar volumes, granule and Purkinje cells in 13 patients diagnosed with MSA [8 MSA-P (striatonigral subtype) and 5 MSA-C (olivopontocerebellar subtype)], 12 PD patients, and 15 age-matched control subjects. Only brains from MSA-C patients showed a reduction in the total number of Purkinje cells (anterior lobe) whereas both MSA-P and MSA-C patients had reduced Purkinje cell volumes (perikaryons and nuclei volume). The cerebellum of both diseases showed a reduction in the white matter volume compared to controls. The number of granule cells was unaffected in both diseases. Analyses of cell type-specific mRNA expression supported our structural data. This study of the cerebellum is in line with previous findings in the cerebrum and demonstrates that the degree of morphological changes is more pronounced in MSA-C than MSA-P and PD. Further, our results support an explicit involvement of cerebellar Purkinje cells and white matter connectivity in MSA-C > MSA-P and points to the potential importance of white matter alterations in PD pathology.

INTRODUCTION

The parkinsonian syndromes are adult-onset neurodegenerative disorders characterized by progressing parkinsonism together with a range of other clinical features. They are neuropathologically classified on a molecular basis as either predominantly synucleinopathies or tauopathies. The synucleinopathies comprise idiopathic Parkinson's disease (PD), dementia with Lewy bodies (DLB), and multiple system atrophy (MSA) (13, 15, 49). In idiopathic PD and DLB, aggregates of conformational posttranslational modifications of the protein α-synuclein (α-syn) accumulate in neurons as Lewy bodies, whereas MSA is characterized by insoluble α-syn-positive glial cytoplasmic inclusions (GCIs) located within oligodendrocytes (12, 18, 22).

Loss of populations of subcortical neurons occurs in idiopathic PD (11), but the total number of neurons is unaffected in the neocortex and hippocampus (24, 40). Findings of cellular changes in the cerebellum of PD patients have been inconsistent (6, 13, 17, 33, 52). However, the phenomenology of PD may predict some involvement of the cerebellum, which plays important roles in the coordination of voluntary movements as well as in gait, balance, and posture, while also contributing to aspects of cognitive functions (4, 30). Indeed, the presence of α-syn pathology has now been demonstrated in the cerebellum of idiopathic PD brains (46), whereas semi-quantitative studies of cerebellar morphology have reported significantly reduced cerebellar volumes (5, 35, 53).

Cerebellar pathology is well-documented in MSA patients. The differing symptom profiles of these subtypes largely concur with the predominant pathologies of striatonigral (MAS-P) or olivopontocerebellar (MSA-C) degeneration (1, 19, 22, 36). Whereas previously published semi-quantitative studies have shown variable degrees of neuronal loss in MSA (1, 13, 36, 49), recent stereological data demonstrate

substantial and region-specific loss of neurons in the basal ganglia, cortex, and white matter of MSA brains (34, 44, 45). Furthermore, these studies show an increased number of microglia, indicating the involvement of neuroinflammatory mechanisms in MSA pathology. Studies focusing on cerebellar morphology in MSA show significantly reduced volumes and Purkinje cell densities in disparate subregions of the cerebellum and brain stem (17, 29, 31, 38, 39, 50).

This literature notwithstanding, no previous stereological studies have been performed to estimate absolute cell numbers and volumes of the cerebellum and its subregions in parkinsonian syndromes. Therefore, we aimed to use design-based stereology to obtain unbiased estimates of the total numbers of Purkinje and granule cells in the four main subregions of the cerebellum (anterior lobe, posterior lobe, vermis, and flocculonodularis) from 12 patients with PD, 13 patients with MSA (8 MSA-P and 5 MSA-C), and 15 age-matched control subjects. Further, we estimated the mean volumes of the Purkinje cell perikarya and nucleus, and of the four cerebellar subdivisions as well as the volume of associated white matter and the dentate nucleus. This stereological quantification was supplemented with molecular biological analysis of cell type-specific markers for Purkinje and granule cells.

MATERIALS AND METHODS

Patients

We used cerebellar hemispheres from 13 MSA patients [MSA-P: 4M/4F, mean age = 66 (60–71) years; MSA-C: 2M/3F, mean age = 63 (61–65) years] and 12 PD patients [7M/5F, mean age = 72 (62–88) years], and 15 neurologically healthy controls [7M/8F, mean age = 69 (56–89) years]. The brains had been obtained from autopsied individuals following the Danish laws on autopsied human tissue, and prior to death, all subjects had given their informed consent. The MSA-P and MSA-C mean brain weights was 1386 (1276–1505) g and 1333 (1246–1550) g, postmortem interval (PMI) = 53 (24–115) hours and 43 (22–95) hours, respectively; the mean PD brain weight was 1320 (1120–1420) g, PMI = 46 (24–118) hours; and the mean control brain weight was 1352 (1040–1580) g, PMI = 36 (10–120) hours. Brains from some of the MSA patients and control subjects have been included in previous studies (2, 3, 25, 44, 45). Frozen cerebellar tissue was used for mRNA expression analysis.

Clinical characteristics are summarized in Table 1 (MSA-P), Table 2 (MSA-C), and Table 3 (PD), and data were

Table 1. Clinical characteristics of patients with MSA-P. Abbreviations: MRI = magnetic resonance imaging, NA = not available, % = percentage of the most frequent categorial variable, SD = standard deviation.

	1	2	3	4	5	6	7	8	Mean (SD) or %
Age at disease onset (years)	57	50	60	55	58	62	63	67	59 (5.2)
Disease duration (years)	5	10	5	6	10	7	7	7	7.1 (2.0)
Cerebellar signs									
Cerebellar dysarthria	−	+	−	−	−	+	+	+	50%
Oculomotor dysfunction*	+	+	−	−	−	+	−	−	63%
Gait ataxia[†]	+	−	+	−	+	−	+	−	50%
Limb ataxia[‡]	−	−	+	−	+	−	−	−	75%
Kinetic or postural tremor	+	+	+	+	+	+	−	−	75%
Parkinsonism[§]	++	++	++	++	++	++	++	++	100%
Autonomic failure[¶]	++	++	++	++	++	++	++	++	100%
Pathological laughter or crying	+	−	+	+	−	+	−	+	63%
Global cognitive impairment**	+	−	−	+	−	−	−	−	75%
Executive dysfunction[††]	+	−	+	+	+	+	−	+	75%
Wheelchair state (years)[‡‡]	3	8	3	3	10	5	*	6	5.4 (2.8)
Positive red-flag categories[§§]	6	4	6	6	1	6	3	5	4.6 (1.8)
Abnormal DAT SPECT	+	+	+	+	+	+	+	+	100%
Cerebellar atrophy in MRI	NA	−	−	−	−	−	−	−	100%

*Oculomotor dysfunction: + = dysmetric saccades and nystagmus.

[†]Gait ataxia: + = wide-based staggering gait.

[‡]Limb ataxia: + = heel-to-shin or finger-to-nose test with dysmetria and decomposition of movements.

[§]Parkinsonism: + = bradykinesia or rigidity, ++ = both.

[¶]Autonomic failure: + = orthostatic hypotension or urinary incontinence, ++ = both.

**Global cognitive impairment: = 125 ≤ Mattis Dementia Rating Scale score ≤ 129. No global cognitive impairment: = either Mattis Dementia Rating Scale score ≥ 130, Addenbrooke's Cognitive Examination (ACE) score ≥ 86, or mini-mental state examination score ≥ 24. All the patients were tested according to the Danish version of ACE (16, 32, 47).

[††]Executive dysfunction: + = impairment of executive function assessed by a neuropsychologist using a battery of frontal assessment tests (including test of verbal fluency (s-words and animals), Stroop Color and Word Test, Wisconsin Card Sorting Test, and Lurias motor series) (14).

[‡‡]Wheelchair state = time from disease onset to wheelchair-bound state.

[§§]Positive red-flag categories: early instability, rapid progression, abnormal postures, bulbar dysfunction, respiratory dysfunction, and emotional incontinence. A category is positive if one or more symptoms within the category are present (28).

*Never reached a wheelchair-bound state.

Table 2. Clinical characteristics of patients with MSA-C. Abbreviations: MRI = magnetic resonance imaging, NA = not available, % = percentage of the most frequent categorial variable, SD = standard deviation.

	1	2	3	4	5	Mean (SD) or %
Age at disease onset (years)	54	60	61	62	55	58 (3.6)
Disease duration (years)	8	3	5	7	6	5.8 (1.9)
Cerebellar signs						
Cerebellar dysarthria	+	+	+	+	+	100%
Oculomotor dysfunction*	+	+	+	−	+	80%
Gait ataxia†	+	+	+	+	+	100%
Limb ataxia‡	+	+	+	+	+	100%
Kinetic or postural tremor	+	−	−	−	−	80%
Parkinsonism§	++	+	+	++	+	60%
Autonomic failure¶	++	++	++	+	++	80%
Pathological laughter or crying	−	−	−	−	−	100%
Global cognitive impairment**	−	NA	−	−	−	100%
Executive dysfunction††	−	NA	−	+	−	75%
Wheelchair state (years)‡‡	7	3	4	6	3	4.6 (1.8)
Positive red-flag categories§§	4	3	3	4	4	3.6 (0.5)
Abnormal DAT SPECT	+	−	+	+	+	80%
Cerebellar atrophy in MRI	+	+	+	+	−	80%

*Oculomotor dysfunction: + = dysmetric saccades and nystagmus.

†Gait ataxia: + = wide-based staggering gait.

‡Limb ataxia: + = heel-to-shin or finger-to-nose test with dysmetria and decomposition of movements.

§Parkinsonism: + = bradykinesia or rigidity, ++ = both.

¶Autonomic failure: + = orthostatic hypotension or urinary incontinence, ++ = both.

**Global cognitive impairment: = $125 \leq$ Mattis Dementia Rating Scale score ≤ 129. No global cognitive impairment: = either Mattis Dementia Rating Scale score ≥ 130, Addenbrooke's Cognitive Examination (ACE) score ≥ 86, or mini-mental state examination score ≥ 24. All the patients were tested according to the Danish version of ACE (16, 32, 47).

††Executive dysfunction: + = impairment of executive function assessed by a neuropsychologist using a battery of frontal assessment tests (including test of verbal fluency (s-words and animals), Stroop Color and Word Test, Wisconsin Card Sorting Test, and Lurias motor series) (14).

‡‡Wheelchair state = time from disease onset to wheelchair-bound state.

§§Positive red-flag categories: early instability, rapid progression, abnormal postures, bulbar dysfunction, respiratory dysfunction, and emotional incontinence. A category is positive if one or more symptoms within the category are present (28).

retrospectively obtained from the patient's medical records. PD brains were obtained between 1958 and 2018, MSA brains from 2007 to 2011, and controls from 1979 to 1989. All MSA patients were diagnosed and followed by movement disorders specialists. MSA patients were clinically diagnosed with probable MSA (either the parkinsonian or cerebellar subtype) according to the recent clinical consensus criteria (19). All PD patients were diagnosed by a movement disorder specialist. Diagnosis and treatment were according to the standard clinical practice at the time of brain donation.

Neuropathology

Tissue samples were taken from the substantia nigra, striatum, cerebral cortex, dentate nucleus, and cerebellar cortex of each MSA and control brain. Tissue blocks were embedded in paraffin and sliced into 5-μm-thick sections for hematoxylin and eosin (HE) staining and immunohistochemistry, including staining for β-amyloid (M0872, 1:1000, DAKO, DK), tau (A0024, 1:1000, DAKO, DK), ubiquitin (Z0458, 1:5000, DAKO, DK), and α-synuclein (sc-12767, 1:9000, Santa Cruz Biotechnologies, US). Additionally, 8-μm-thick sections were cut for Klüver–Berrara staining. The neuropathological examination showed no overall vasculitis, encephalitis, tumors or neuronal and glial inclusions in the control subjects. Definite diagnoses were confirmed based on the presence of GCIs, gliosis, and neuronal loss in MSA patients (48). Occurrence of Lewy bodies and a notable loss of pigmented neurons in the substantia nigra were described in all brains from PD patients. Following brain donation, neuropathology in the substantia nigra was available in 11 out of the 12 PD patients. The last patient was diagnosed on clinical signs only, since the substantia nigra was kept for research purposes due to the patient having received deep brain stimulation.

Cerebellar anatomy

The cerebellum was divided into four major anatomical subdivisions as previously described (10): the anterior and posterior lobes (pontocerebellum), vermis (spinocerebellum), and the flocculonodular lobe (vestibulocerebellum). Functionally, these subregions are primarily engaged with the following motor pathways and functions: The pontocerebellum is connected primarily to the cerebral motor cortex via the thalamus and is primarily involved in coordination of movements; the spinocerebellum mediates muscle tone and bodily posture through its connections to the red nucleus, and the vestibulocerebellum mediates balance through its connections to the vestibular system. The cerebellar cortex consists of three layers, the outer molecular layer, the middle Purkinje cell layer, and the inner granule cell layer. The sole output of the cortex is the projections of the Purkinje cells to the deep nuclei, which in turn give rise to most of efferent fibers from the cerebellum (51).

Tissue processing

The tissue processing was performed as previously described with minor modifications (2). In brief, all brains were fixed within a mean of 44 ± 32 hours after death and stored in fixative (10% neutral buffered formalin, pH = 7.2) for at least one month. The cerebellum was dissected from the brain stem and its surface painted with waterproof ink to distinguish

Table 3. Clinical characteristics of patients with PD. In addition to the above-mentioned treatment, patient five received orphenadrine whereas patient ten and eleven received dopa-agonists and entacapone. Abbreviations: As = arteriosclerosis, BS = babinski signs, D = dementia, Dp = depression, GAp = global aphasia, GAt = global ataxia, L = left, NA = not available, % = percentage of the most frequent categorial variable, PT = postural tremor, R = right, S = symmetric, SD = standard deviation, SF = Spanish flu, Sp = spasticity, Spi = lumbar spinal stenosis, St = stroke, TIA = transient ischemic attack, U = universal.

PD	1	2	3	4	5	6	7	8	9	10	11	12	Mean (SD) or %
Age at disease onset (years)	71	57	68	72	68	59	66	45	87	52	51	61	63 (11)
Disease duration (years)	3	5	1.5	2	6	13	5	26	0.5	19	13	11	8.8 (7.9)
Motor symptoms													
Rigidity	U	U	S	R	L > R	R > L	S	S	R	R > L	R > L	S	33%
Bradykinesia	–	S	S	S	–	S	–	R	–	S	R > L	S	50%
Tremor	–	PT	–	R > L	–	R > L	+	–	–	R > L	R > L	L	42%
Postural instability	–	+	+	+	–	–	+	–	–	–	–	+	58%
Oligemia	+	+	–	–	+	+	+	+	–	+	+	+	75%
Hypophonia	+	–	–	–	–	+	+	–	–	+	+	+	50%
Parkinsonian gait	–	–	–	–	–	+	+	+	–	+	+	+	50%
Gait freezing	–	–	–	+	–	–	+	–	–	+	–	–	75%
Cognition	D	NA	NA	D	NA	D	D	D	–	–	D	D	70%
Treatment	NA		NA	NA									
Amantadine		–			–	+	+	+	–	–	–	–	67%
Bromocriptine		–			–	+	–	–	–	–	–	–	89%
Levodopa		–			–	+	+	+	+	+	+	+	78%
Pergolide		–			–	–	–	–	–	+	–	–	89%
Selegilin		–			–	–	–	–	–	–	–	+	89%
Trihexyphenidyl		+			–	–	+	–	–	–	–	–	78%
Surgery/year		–			–	–	–	1965	–	2004	–	–	78%
Duodopa		–			–	–	–	–	–	–	2012	–	89%
Response to treatment		+			NA	+	+	+	NA	+	+	+	100%
Side effects (hallucination, dyskinesia)		NA			NA	+	NA	+	NA	+	+	–	80%
Comorbidity	As	SF	NA	SF	NA	NA	St	NA	TIA	NA	Spi	St, DP	29%
Co-occurring neurological signs and symptoms	GAt, BS	Sp	NA	NA	GAp	NA	NA	NA	NA	NA	–	GAp	40%

the four subdivisions. After removing the flocculonodular lobe, the remaining cerebellum was embedded in 4% agar and sliced systematically into 4.0-mm-thick slabs with a random starting point within the slab thickness. The flocculonodular lobe was embedded in 4% agar and cut into 2.0-mm-thick slabs. All slabs were photographed for estimating the volume of each cerebellar region. Then, the slabs were cut systematically into 4-mm-wide columns or rods, and every 3th rod was subsampled. The sampled rods were dehydrated and, after being randomly rotated around the vertical axis, embedded in Historesin (2-hydroxyethyl methacrylate), whereupon a central 40-μm-thick section was cut and stained with a modified Giemsa stain. During the preparation of the rods, extra rods were sampled to measure shrinkage before and after processing. No net shrinkage was detected.

Stereological methods

In the four cerebellar regions, we delineated the region of interest in each section through a 2× objective. Estimation of volumes was performed using Cavalieri's point-counting principle (21). Applying optical disectors (20), we estimated the numerical densities of Purkinje and granule cells using the CAST software (Visiopharm, Hørsholm, DK), with imaging by an Olympus BX51 microscope and a motorized stage.

Purkinje cells were estimated using a 60× oil-immersion objective (numerical aperture (NA) = 1.40) at a final magnification of 1000×, and granule cells with a 100× oil-immersion objective (NA = 1.35) at 1670x magnification. Rectangular counting frames measuring 80 μm^2 for granule cells and 28 000 μm^2 for Purkinje cells were superimposed on the magnified image of the tissue projected onto a computer screen, and movements in the z-direction were measured with a digital microcator (Heidenhain, VRZ 401). The average section thickness was 40 μm, resulting in a 5-μm guard zone at the top of the section, a disector height of 15-μm and a 20-μm guard zone in the bottom of the disector. We identified Purkinje cells based on their large, clear nucleus with a deeply stained nucleolus and irregular Nissl granules; the Purkinje cell nucleolus was used as the counting item, or, in its absence, the nucleus; granule cells were identified by their location in the densely packed granular layer in which they reside, and by their dark nucleus, which nearly fills the cell body (Figure 1). Using step lengths of 1700 μm and 600 μm, we counted means of 145 (range 33–374) granule cells in 54 (range 18–122) fields of view and 122 (range 34–186) Purkinje cells in 745 (range 172–2090) fields of view in each cerebellar subregion. A uniform distribution of neurons within the disector height was confirmed by analyzing the z-distribution of particles. We used a mean of
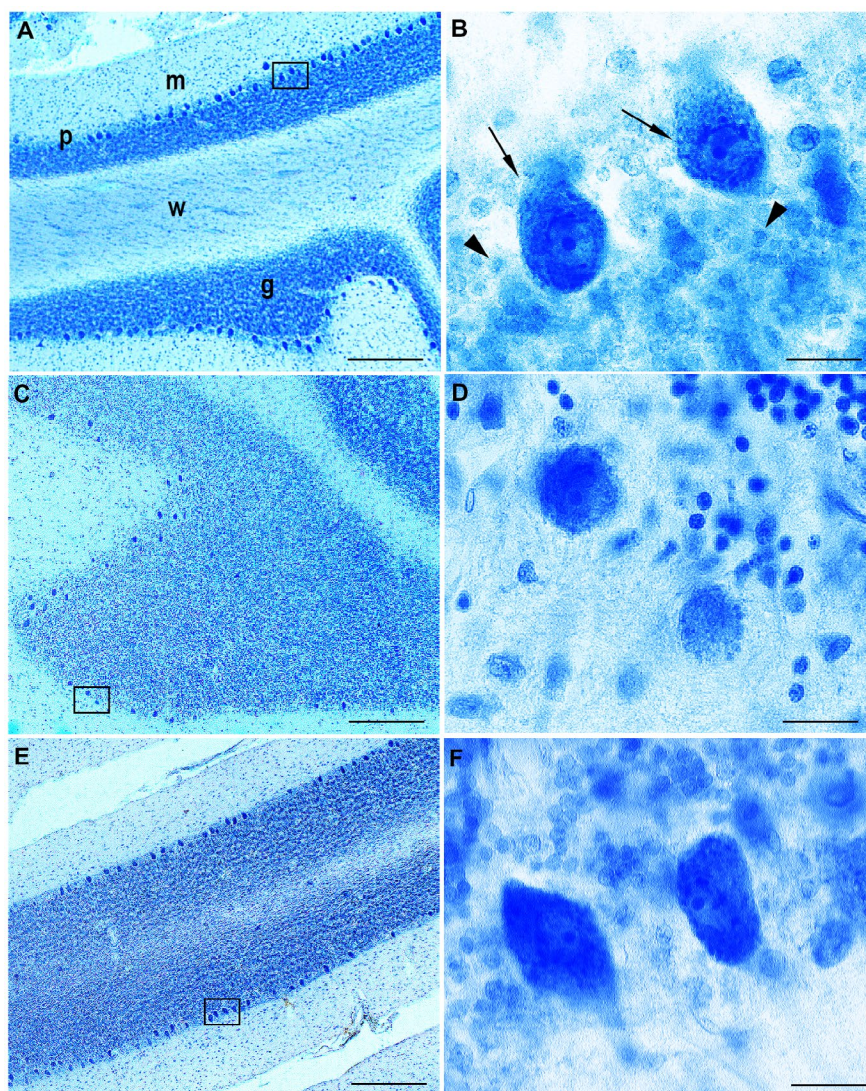
Figure 1. Micrographs showing Giemsa stained sections of the anterior lobe at ×4 magnification (A, C, E; scale bar = 375 µm) and ×60 magnification (B, D, F: scale bar = 25 µm) in control (A, B), MSA (C, D), and PD brains (E, F). Arrows = Purkinje cell, arrowheads = granule cell, g = granule cell layer, m = molecular layer, p = Purkinje cell layer, and w = white matter.

20 (range 13–30) sections per cerebellum for cell counting, and the total number of each cell type was finally calculated by multiplying their numerical density by the reference volume, with doubling to obtain bilateral numbers.

We measured the volumes of Purkinje cell nuclei and perikaryons using the vertical rotator principle (23). The mean number of Purkinje cells used for volume estimations was 75 (30–240) per cerebellar region.

qRT-PCR

Frozen cerebellar tissue from the full height of the cortex in the anterior (equal to lobule IV) and posterior (equal to crus II) lobes in seven control subjects, nine MSA (P + C), and six PD patients (clinical data not shown) were collected for comparison of mRNA levels (qRT-PCR) of specific markers for Purkinje cells (Calb1), granule cells (VGLUT1 and NeuroD1), and neurons in general (NeuN). The qRT-PCR procedure was performed as described in detail elsewhere (45). In brief, RNA was extracted from 50-mg samples using the RNeasy Mini purification kit (Qiagen, DEU). The RNA integrity and quantity were assessed using the Agilent 2100 Bioanalyzer (Agilent Technologies, US) before the samples were stored at −80°C until further processing. The following primer pairs (5′-3′) were used to measure the mRNA expression levels of Calb1 (Sense: GGCTCCATTTCGACGCTGA, antisense: AACTTTTGTGGATCAGTATGGGC), VGLUT1 (Sense: CGACGACAGCCTTTTGTGGT, antisense: CTCTGT TTTCTACGTCTACGGC), NeuroD1 (Sense: GGATGACG ATCAAAAGCCCAA, antisense: TGCCTTGCTATTCTAA

GACGC) and NeuN (Sense: TCAATAATGCCACGGCCCGA GTGA, antisense: GCTAAATCCAGTGGTCGGCGCAGT), which were normalized to the expression levels of hGAPDH, hATP5B, hPPIA, and hUBE2D2 (43) using a comparative cycle of threshold fluorescence method. The qRT-PCR reactions were performed using Fast SYBR Green Master Mix (Applied Biosystems, US), and the results are expressed as relative quantity to the calibrator sample using the Pfaffl method (41).

Statistics

Stereological data and mRNA expression levels were analyzed using one-way ANOVA followed by Tukey's multiple comparisons test. When normality distribution failed (Shapiro–Wilk normality test), we applied Kruskal–Wallis tests followed by Dunn's multiple comparisons test. For analyses of the average volume distribution of Purkinje cell perikarya and nucleus, we performed 2-way ANOVA followed by Tukey's

multiple comparisons test. The biological variances, expressed as the coefficient of variance (CV), of the total number of Purkinje and granule cells, the volume of Purkinje cell nuclei and perikaryons, and cerebellar subdivisions are shown in Tables 4–6, respectively. The precision of the estimates of total cell numbers, expressed as the coefficient of error (CE), are shown in Table 4. Outliers were excluded when data points fell outside the range of mean ± 2 x standard deviations. Data analysis and graphical presentation were completed using GraphPad Prism 8 software (GraphPad Software Inc., USA). The level of significance was set at $P < 0.05$.

RESULTS

Total number of Purkinje cells

In MSA (P + C) brains, the total number of Purkinje cells (Table 4) was significantly reduced by 36% in the anterior

Table 4. Numerical estimation of the mean total number of Purkinje and granule cells in the cerebellum of control subjects and patients with MSA and PD. Please note that total volumes do not always apply to the sum of the subregions because of outlier removal. CV values (standard deviation/mean) represented in parenthesis. Abbreviations: C = cerebellar subtype of MSA, CS = control, MSA = multiple system atrophy, P = Parkinsonian subtype of MSA, PD = Parkinson's disease, and FlocNod = flocculonodularis.

	CS	CE	PD	CE	MSA (P + C)	CE	MSA-P	CE	MSA-C	CE
Purkinje cell number (10^6)										
Anterior	2.63 (0.35)	0.09	2.25 (0.32)	0.08	1.68 (0.38)*	0.10	2.15 (0.39)	0.10	1.34 (0.44)*	0.09
Posterior	18.02 (0.27)	0.08	17.31 (0.24)	0.09	16.05 (0.21)	0.09	17.83 (0.16)	0.09	13.55 (0.18)	0.09
Vermis	1.88 (0.28)	0.09	1.99 (0.25)	0.08	1.50 (0.45)	0.10	1.59 (0.50)	0.10	1.34 (0.33)	0.10
FlocNod	0.40 (0.58)	0.10	0.46 (0.32)	0.09	0.38 (0.22)	0.11	0.48 (0.36)	0.11	0.36 (0.35)	0.11
Total	22.75 (0.26)		22.10 (0.20)		19.77 (0.20)		19.43 (0.13)		16.45 (0.15)	
Granule cell number (10^9)										
Anterior	8.75 (0.28)	0.08	9.45 (0.40)	0.07	7.58 (0.40)	0.09	8.75 (0.30)	0.09	5.69 (0.49)	0.09
Posterior	73.45 (0.16)	0.08	82.20 (0.08)	0.06	74.83 (0.27)	0.07	78.77 (0.27)	0.07	68.54 (0.27)	0.07
Vermis	6.22 (0.22)	0.08	7.05 (0.23)	0.07	7.80 (0.50)	0.09	8.48 (0.49)	0.09	6.71 (0.52)	0.09
FlocNod	0.83 (0.47)	0.11	1.20 (0.40)	0.11	0.90 (0.22)	0.10	1.19 (0.53)	0.12	0.82 (0.26)	0.13
Total	89.85 (0.14)		101.90 (0.08)		90.94 (0.25)		96.89 (0.25)		81.43 (0.25)	

*$P < 0.05$ vs. control.

Table 5. Estimation of mean volume of Purkinje cell nucleus and perikarya in control subjects and patients with MSA and PD. Please note that total mean volumes do not always apply to the mean of the subregions because of outlier removal. CV values (standard deviation/mean) are represented in parenthesis. Abbreviations: C = cerebellar subtype of MSA, CS = control, MSA = multiple system atrophy, P = Parkinsonian subtype of MSA, PD = Parkinson's disease, and FlocNod = flocculonodularis.

	CS	PD	MSA (P + C)	MSA-P	MSA-C
Nucleus (μm^3)					
Anterior	1578 (0.12)	1636 (0.12)	1103 (0.27)***,###	1117 (0.23)**,###	1080 (0.37)**,##
Posterior	1603 (0.14)	1516 (0.08)	1198 (0.27)*	1148 (0.29)*	1279 (0.25)
Vermis	1555 (0.18)	1479 (0.18)	1248 (0.21)*	1231 (0.19)	1271 (0.27)
FlocNod	1453 (0.12)	1518 (0.12)	1154 (0.11)*,##	1171 (0.09)#	1127 (0.17)
Total	1501 (0.16)	1583 (0.11)	1214 (0.20)*,##	1203 (0.18)*,##	1232 (0.25)#
Perikarya (μm^3)					
Anterior	16278 (0.12)	15627 (0.12)	9932 (0.28)***,###	10805 (0.36)***,##	10183 (0.32)***,##
Posterior	17044 (0.17)	15148 (0.13)	11017 (0.20)***,##	11425 (0.28)***,#	11678 (0.22)**
Vermis	17169 (0.15)	14494 (0.11)	11443 (0.25)***	12541 (0.31)**	11205 (0.26)**
FlocNod	14114 (0.14)	14637 (0.16)	11512 (0.16)#	12005 (0.14)	10690 (0.20)
Total	16135 (0.12)	15222 (0.12)	11070 (0.19)***,###	11786 (0.25)***,#	11230 (0.23)***,#

*$P < 0.05$ vs. CS; **$P < 0.01$ vs. CS; ***$P < 0.001$ vs. CS; #$P < 0.05$ vs. PD; ##$P < 0.01$ vs. PD; ###$P < 0.001$ vs. PD.

Table 6. Estimation of cerebellar volumes (cm^3) in control subjects and patients with MSA and PD. Please note that total cerebellar volumes do not always apply to the sum of the subregions because of outlier removal. CV values (standard deviation/mean) are represented in parenthesis. Abbreviations: C = cerebellar subtype of MSA, CS = control, MSA = multiple system atrophy, P = Parkinsonian subtype of MSA, PD = Parkinson's disease, and FlocNod = flocculonodularis.

	CS	PD	MSA (P + C)	MSA-P	MSA-C
Cerebellar cortex					
Anterior	8.41 (0.24)	8.27 (0.33)	7.25 (0.24)	7.64 (0.22)	6.61 (0.27)
Posterior	64.72 (0.18)	68.87 (0.09)	65.50 (0.17)	68.55 (0.15)	60.64 (0.19)
Vermis	7.52 (0.11)	7.16 (0.09)	6.95 (0.27)	7.55 (0.26)	7.66 (0.56)
FlocNod	0.87 (0.38)	1.20 (0.19)	1.17 (0.18)	1.37 (0.29)*	1.11 (0.21)
Total	81.44 (0.16)	85.88 (0.08)	81.16 (0.16)	84.65 (0.14)	75.57 (0.18)
Granule cell layer					
Anterior	3.92 (0.29)	3.67 (0.34)	3.63 (0.29)	3.80 (0.28)	3.36 (0.34)
Posterior	28.38 (0.17)	30.45 (0.09)	30.74 (0.16)	30.11 (0.15)	30.15 (0.19)
Vermis	3.30 (0.18)	3.24 (0.17)	3.50 (0.27)	3.74 (0.29)	4.02 (0.57)
FlocNod	0.46 (0.37)	0.59 (0.26)	0.57 (0.17)	0.66 (0.32)	0.57 (0.20)
Total	35.97 (0.14)	38.75 (0.05)	38.62 (0.14)	39.09 (0.14)	37.87 (0.17)
Molecular layer					
Anterior	4.49 (0.23)	4.61 (0.34)	3.62 (0.23)	3.84 (0.23)	3.25 (0.21)
Posterior	35.55 (0.19)	39.30 (0.10)	34.76 (0.20)	37.43 (0.18)	30.49 (0.20)
Vermis	4.18 (0.14)	3.93 (0.12)	3.46 (0.28)	3.81 (0.25)	3.63 (0.57)
FlocNod	0.43 (0.43)	0.61 (0.20)	0.65 (0.28)*	0.71 (0.27)*	0.54 (0.22)
Total	44.59 (0.18)	48.72 (0.08)	41.15 (0.17)	45.56 (0.17)	37.70 (0.17)#
White matter	30.03 (0.26)	21.05 (0.26)*	18.09 (0.43)***	22.53 (0.20)	11.00 (0.56)***
Dentate nucleus	1.92 (0.21)	2.08 (0.28)	1.41 (0.41)	1.54 (0.41)	1.13 (0.38)

*$P < 0.05$ vs. CS; ***$P < 0.001$ vs. CS; #$P < 0.05$ vs. PD.

lobe ($P = 0.02$, Figure 2B) with no differences in the entire cerebellum (Figure 2A), the posterior lobe (Figure 2C), the vermis (Figure 2D), or the flocculonodularis (Figure 2E), when compared to the control group. Within-group analysis showed that MSA-C brains had a significant lower number of Purkinje cells in the anterior lobe ($P = 0.02$) compared to controls, with no differences in the other subregions or the entire cerebellum. The total number of Purkinje cells in MSA-P patients did not differ significantly from MSA-C or control brains. We saw no significant changes in the total number of Purkinje cells in PD brains compared to controls in any of the four subregions, nor did the total number of the Purkinje cells differ in the entire cerebellum. Additionally, Purkinje cell counts did not differ between MSA groups and PD brains.

Volume of Purkinje cell nucleus and perikarya

Estimation of Purkinje cell volumes in the cerebellum of MSA (P + C) patients showed a significantly smaller mean volume of the nucleus (19%) and perikarya (31%) in all regions compared to controls (Table 5). We also saw a significantly 23% smaller mean nucleus volume and 27% smaller perikarya volume in the total cerebellum of MSA (P + C) compared to PD brains, with no difference in cell volumes in the posterior lobe (nucleus) and vermis (nucleus and perikarya). No significant differences were observed in the nucleus or perikarya volumes between MSA-C and MSA-P, or PD and control brains.

Scatter plots of the size distribution of Purkinje cells in the entire cerebellum of MSA (P + C), PD, and control brains are shown in Figure 2F-G. In general, cerebella from

MSA (P + C) patients had more Purkinje cells with reduced nuclear volume (Figure 2F), a difference which was significant for volumes of 600–800 μm^3 ($P < 0.05$). There were also fewer Purkinje cells with larger nuclear sizes (1000–2000 μm^3 and 2000–3000 μm^3; $P < 0.0001$), and likewise fewer cells with larger perikarya volume (10 000–20 000 μm^3 and 20 000–30 000 μm^3; $P < 0.0001$, Figure 2G), but no significant differences were observed in the small Purkinje cells with parikarya volume <10 000 μm^3. Finally, the total number of Purkinje cells with a nuclear volume between 1000 and 2000 μm^3 and a perikarya volume between 20 000 and 30 000 μm^3 was significantly lower in PD brains ($P < 0.05$ and $P < 0.01$, respectively), compared to controls.

Total number of granule cells

The total number of granule cells in the entire cerebellum and its subregions are shown in Table 4. Compared to control subjects, granule cell numbers in MSA (P + C) brains did not significantly differ in the entire cerebellum or any of its four subregions, nor did the numbers in PD brains. Neither did MSA (P + C) brains show any significant differences when compared to PD brains. No differences in the total number of granule cells between MSA-P and MSA-C brains were observed in any subregion, nor were there any differences when compared to brains from control or PD patients.

Volume of cerebellum and its subdivisions

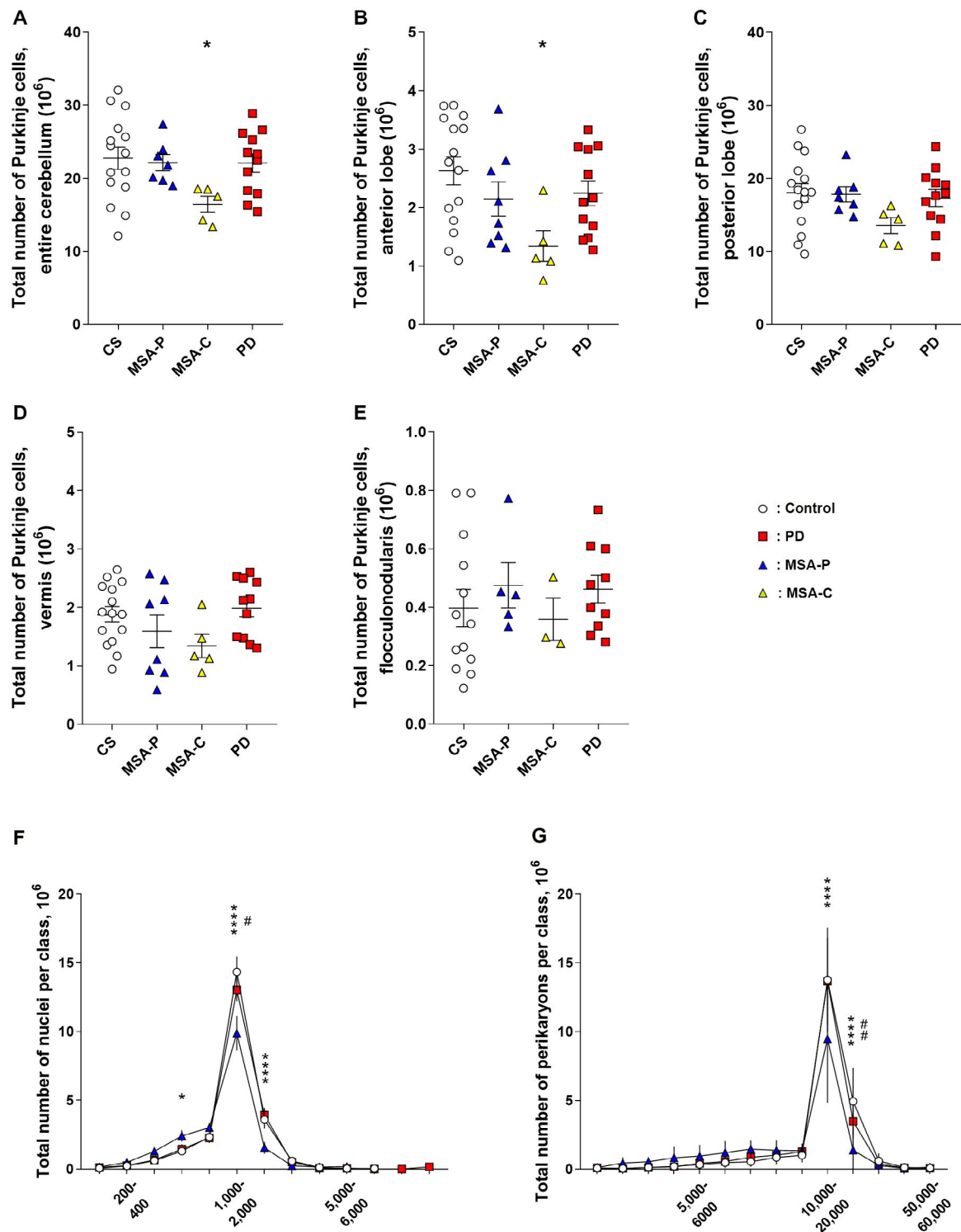The mean volumes of the cortex and cortical layers in the entire cerebellum and its subregions are shown in

Figure 2. Total number of cerebellar Purkinje cells in the entire cerebellum (A), anterior lobe (B), posterior lobe (C), vermis (D) and flocculonodularis (E) and average size distribution of the nucleus (μm^3, F) and perikarya (μm^3, G). *$P < 0.05$ (CS vs. MSA), ****$P < 0.0001$ (CS vs. MSA), #$P < 0.05$ (CS vs. PD), and ##$P < 0.01$ (CS vs. PD).

Table 6. The entire cerebellum had a mean volume of 113 cm^3 (CV = 0.17) in control brains, 101 cm^3 (CV = 0.18) in MSA (P + C) brains, 108 cm^3 (CV = 0.14) in MSA-P brains, 87 cm^3 (CV = 0.17) in MSA-C brains, and 110 cm^3 (CV = 0.05) in PD brains ($P = 0.02$). Post hoc test showed that the cerebellar volume of MSA-C brains was

significantly lower than control (*P* = 0.02). Neither the total cerebellar cortex nor its two major layers (granular and molecular layers) showed significant differences between MSA groups, PD, and controls, except in the total volume of the molecular layer which was significantly lower in MSA-C (*P* = 0.04) when compared to PD. The white matter volume was significantly 40% lower in MSA (P + C), 63% lower in MSA-C, and 30% lower in PD brains compared to controls. Furthermore, the cerebellar white matter volume was significantly 51% lower in MSA-C than MSA-P brains. No differences were observed in the volume of the dentate nucleus when comparing MSA, PD, and control groups.

Total volumes of the cerebellar cortex in the four lobes did not differ between MSA groups, PD, and control groups, except in the flocculonodularis, which was significantly larger in the MSA-P group (36%), compared to controls. Subdivision of the lobes into cortical layers showed a greater volume of the molecular layer in the flocculonodularis of MSA (P + C) (34%) and MSA-P brains (40%), compared to controls. The other subdivisions of the cerebellum showed no significant differences.

Validation of results

To validate our results, we compared our stereological data of the total number of Purkinje and granule cells as well as the volumes of the anterior and posterior lobes with previously obtained results from our laboratory (2, 3). These results showed no significant differences between our present data and the results from earlier studies on control subjects (Figure 3A, age group: 56–90 years, Purkinje cells: *P* = 0.20; granule cells: *P* = 0.84 and Figure 3B, age group: 56–90 years,

anterior lobe: *P* = 0.14; posterior lobe: *P* = 0.73). Further, to exclude that white matter changes were caused by levodopa treatment and/or dementia in PD brains we included archive material of white matter volumes from an extra cohort of ten PD patients [7M/3F, mean age = 76 (68–83) years]. No significant differences were found in the volume of the cerebellar white matter between levodopa treated [n = 17, 18.48 (13.72–24.36) cm^3] and non-levodopa treated [n = 5, 19.00 (12.20–23.60) cm^3] brains (*P* = 0.77) or demented [n = 11, 19.91 (15.01–23.60) cm^3] versus non-demented [n = 9, 17.19 (12.20–24.36) cm^3] PD patients (*P* = 0.09).

Analysis of cell marker mRNA levels

The relative mRNA expression levels of Calb1, VGLUT1, NeuroD1, and NeuN by group are shown in Figure 4. Our data show significantly lower levels of the Purkinje cell marker (Calb1) in the anterior lobe of both MSA (P + C) (*P* = 0.019) and PD (*P* = 0.019) patients compared to controls, with no such difference in the posterior lobe (Figure 4A). Furthermore, we did not observe differences from control values in the levels of VGLUT1 (Figure 4B), NeuroD1 (Figure 4C), or NeuN (Figure 4D) in any of the examined cerebellar regions, nor did we observe significant differences in these cell markers in the contrast between MSA (C + P) and PD.

DISCUSSION

The mean number of Purkinje cells in the cerebellum was reduced in the anterior lobe of the MSA (P + C) group compared to controls. Within-group analysis showed that
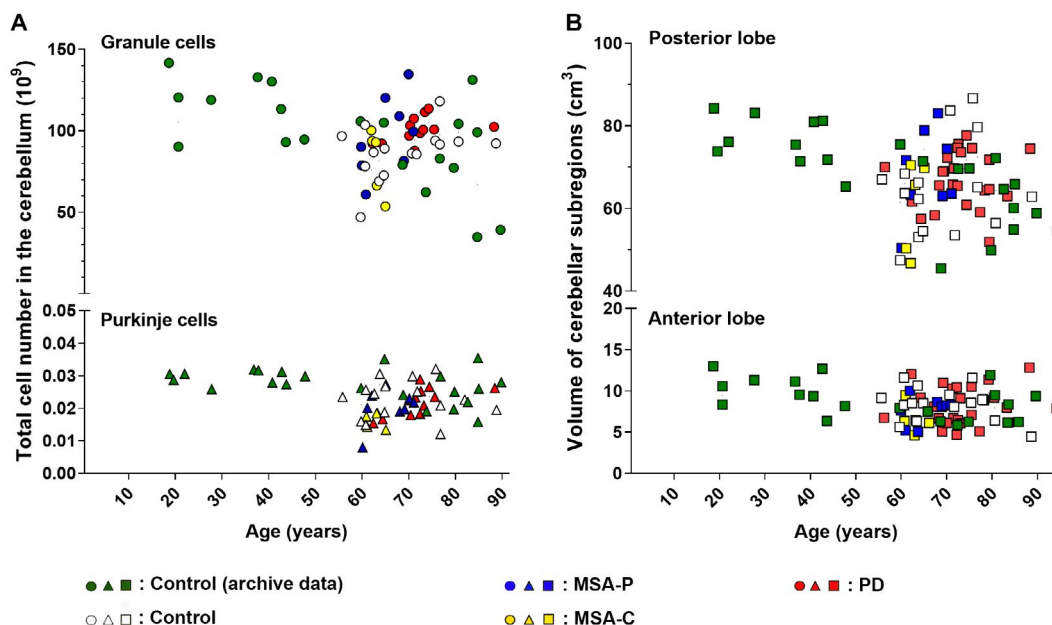

Figure 3. Total number of granule and Purkinje cells (A), and total volumes (B) in the cerebellum as a function of age. Included are stereological archive data from 21 control subjects from our laboratory, and data from eight MSA-P, five MSA-C, 12 PD, and 15 control subjects included in the present study.
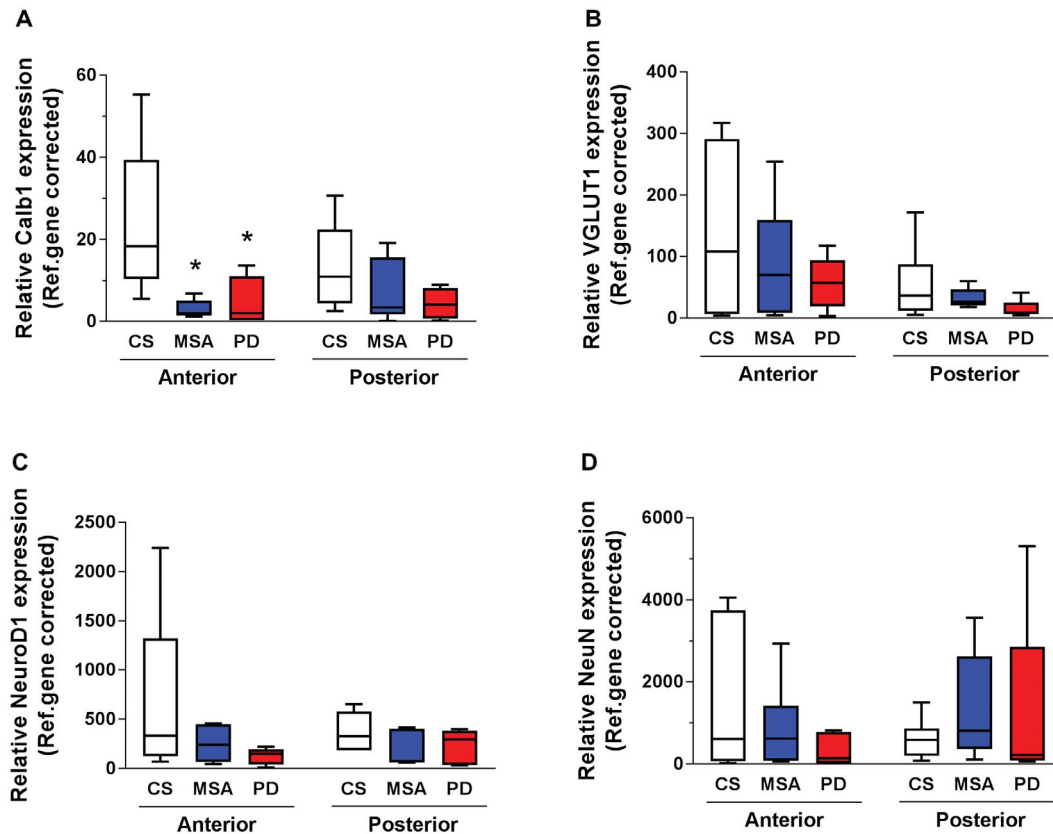
Figure 4. The relative mRNA expression levels of Calb1 (A), VGLUT1 (B), NeuroD1 (C), and NeuN (D) in the anterior and posterior lobes of MSA, PD, and control subjects. CS = control, MSA = multiple system atrophy, PD = Parkinson's disease. *$P < 0.05$ (CS vs. MSA).

the reduced number of Purkinje cells was caused by a significantly lower number in brains from MSA-C patients. These findings in MSA brains are in accordance with previous stereological estimations of the basal ganglia nuclei showing reduction in the total number of neurons and support region-specific patterns of neuronal loss in MSA (44). Cognitive impairment has been documented in approximately 20% of patients with MSA (7) and may be concomitant to cerebellar degeneration (27), especially in the posterior lobes (4, 17). However, we observed no differences in the volume or the total number of neurons (Purkinje or granule cells) in the posterior lobe of MSA brains compared to control subjects. This is consistent with results of previous studies suggesting that cognitive dysfunction in MSA is more related to cerebral cortical pathology (9, 17, 26, 45). The MSA patients who were donors in the present study had shown prominent postural instability, with a mean time from disease onset to wheelchair-dependence of only five years. Indeed, postural instability is a more prominent clinical feature in MSA patients than in PD (19, 49).

Based on recent imaging-based findings of reduced cerebellar volumes in PD (5, 35, 53) and the detection of α-syn pathology in the cerebellum of PD brains (46), cerebellar pathology has been implicated in aspects of the postural instability, tremor, and cognitive dysfunction in PD (17, 52). However, we saw no reduction in the total number

of granule or Purkinje cells, nor were the cell-body volumes reduced in post mortem cerebella from PD patients, which does not support a strong dependence between clinical symptoms and structural gray matter changes in the cerebellum of PD patients.

The white matter volume was reduced in cerebellum of the MSA group (MSA (P + C) = 40%, MSA-C = 63%, MSA-P = 25% (non-significant)), and likewise in the PD group (30%), which stands in contrast with the unaltered cell counts and volumes in PD. However, white matter atrophy in both diseases is consistent with results of previous imaging studies in brains of living MSA (33, 38) and PD patients (5, 35). Thus, compromised cerebellar white matter alterations was a prominent feature of the structural pathology in MSA-C and PD, and to a lesser degree in MSA-P, which plausibly manifests in impaired connectivity within the cerebellum, between the cerebellum and the cerebrum and/or the cerebellum and the brain stem (31). Our findings of no significant volumetric changes in the entire cerebellar cortex or its main subdivisions emphasize the potential importance of cerebellar white matter alterations in MSA and PD pathology and symptomatology. Furthermore, the total number of granule cells, which receive the main *input* to the cerebellum through mossy fibers, was unaffected in the entire cerebellum and its subdivisions in both diseases. The present results support a hypothesis that disrupted

cerebellar *output* via reduced connectivity of inhibitory projections from the cerebellar cortex to the deep nuclei contribute to the pathophysiology of MSA-C, and to a lesser degree, also in MSA-P and PD. Even though the underlying mechanisms of increased pathology in the cerebellum of MSA-C patients are not known, our results are consistent with previous studies describing more severe neuropathological changes in the olivopontocerebellar structures in MSA-C compared to MSA-P (22, 36), and in line with the clinical representation in MSA-C patients (19).

One previous stereological study demonstrated decreasing Purkinje cell perikarya size, but unaffected nuclear size, during normal aging (3). We now demonstrate a significant reduction in the mean volume of Purkinje cell perikaryons and nuclei throughout the cerebellum of MSA patients relative to age-matched controls. Our study of cell size distributions shows that the mean volume loss of Purkinje cells in MSA brains is driven by a greater abundance of small-sized Purkinje cells and lower abundance of large-sized Purkinje cells compared to PD and controls. In summary, these data indicate declines in the number and mean volume of Purkinje cells in MSA brains that are not evident in PD and normal aging, changes that seem apt to result in altered functionality of the deep cerebellar nuclei in MSA.

Our data show decreased mRNA levels of the Purkinje cell marker Calb1 in the anterior, but not the posterior lobe of MSA (P + C) and PD patients. Further, our data did not demonstrate significant alterations in the granule cell markers (VGLUT1 and NeuroD1) or the general neuronal marker (NeuN) in any of the examined regions or patient groups. These results are partly in line with our structural data in showing preservation of granule cells and loss of Purkinje cells in MSA-C cerebella. However, no markers showed any difference in mRNA expression between MSA-P and MSA-C when evaluating the two MSA subtypes descriptively. Further studies are needed to clarify the discrepancy between the number of Purkinje cells and Calb1 mRNA expression in the anterior lobe of the cerebellum from PD and MSA-P patients.

This study has several limitations, one being the small sample sizes in all groups, especially the MSA-C group. Thus, future stereological studies of the cerebellum in these patient groups using larger sample sizes are wanted. To validate our results, we compared our stereological data of the total number of Purkinje and granule cells as well as the volumes of the anterior and posterior lobes with previously obtained results from our laboratory (2, 3). These results showed no significant differences between our present data and the results from earlier studies on control subjects. Second, we concede that shrinkage may occur during histological processing, thereby biasing the volume estimations (but not the cell counting) in this kind of study. However, our adoption of plastic embedding media will result in minimized shrinkage, and furthermore, our sampling of extra rods specifically to measure shrinkage before and after processing did not indicate any net shrinkage. Finally, any differential shrinkage between disease and control brains taking place prior to embedding can never be excluded in a study

such as this. However, the difference in the estimates of Purkinje cell volume (rotator volumes) between control and MSA as well as between MSA and PD have such a magnitude that we regard this possibility less likely.

The major strength of the present study includes the use of design-based stereology. Whereas most former studies applied two-dimensional morphometric and histometric methods, resulting in 2D estimates or estimates based on size distribution of 2D neuronal profiles, we used stereological methods, which are without these limitations. Our stereological data are supported by molecular biology analyses showing parallel changes in mRNA expression using markers specific for these cell types.

In conclusion, although MSA and PD patients share many symptoms, especially in the beginning of the disease, the prognosis is very different, with limited treatment options available for MSA patients. Recent studies have shown that the degree of brain pathology is more severe in MSA than PD (8, 37, 40, 42, 45). Our results in the cerebellum are in line with these findings and may help to pin-point dissimilarities between MSA-C, MSA-P, and PD.

ACKNOWLEDGMENTS

CONFLICT OF INTEREST

Nothing to report.

DATA AVAILABILITY STATEMENT

Requests for materials supporting the findings of this study should be addressed to the corresponding author.

REFERENCES

1. Ahmed Z, Asi YT, Sailer A, Lees AJ, Houlden H, Revesz T, Holton JL (2012) The neuropathology, pathophysiology and genetics of multiple system atrophy. *Neuropathol Appl Neurobiol* **38**:4–24.
2. Andersen K, Andersen BB, Pakkenberg B (2012) Stereological quantification of the cerebellum in patients with Alzheimer's disease. *Neurobiol Aging* **33**:197.e11–197.e20.

3. Andersen BB, Gundersen HJ, Pakkenberg B (2003) Aging of the human cerebellum: a stereological study. *J Comp Neurol* **466**:356–365.

4. Bodranghien F, Bastian A, Casali C, Hallett M, Louis ED, Manto M *et al* (2016) Consensus paper: revisiting the symptoms and signs of cerebellar syndrome. *Cerebellum* **15**:369–391.

5. Borghammer P, Ostergaard K, Cumming P, Gjedde A, Rodell A, Hall N, Chakravarty MM (2010) A deformation-based morphometry study of patients with early-stage Parkinson's disease. *Eur J Neurol* **17**:314–320.

6. Braak H, Braak E (2000) Pathoanatomy of Parkinson's disease. *J Neurol* **247**(Suppl. 2):II3–II10.

7. Brown RG, Lacomblez L, Landwehrmeyer BG, Bak T, Uttner I, Dubois B *et al* (2010) Cognitive impairment in patients with multiple system atrophy and progressive supranuclear palsy. *Brain* **133**:2382–2393.

8. Brudek T, Winge K, Folke J, Christensen S, Fog K, Pakkenberg B, Pedersen LØ (2017) Autoimmune antibody decline in Parkinson's disease and Multiple System Atrophy; a step towards immunotherapeutic strategies. *Mol Neurodegener* **12**:44.

9. Chang CC, Chang YY, Chang WN, Lee YC, Wang YL, Lui CC *et al* (2009) Cognitive deficits in multiple system atrophy correlate with frontal atrophy and disease duration. *Eur J Neurol* **16**:1144–1150.

10. Crossman A, Neary D (2015) Neuroanatomy: an illustrated colour text. Churchill Livingstone: London (UK).

11. Cumming P, Borghammer P. (2012) Molecular Imaging and the Neuropathologies of Parkinson's Disease. In Brain Imaging in Behavioral Neuroscience, CS Carter, JW Dalley (eds), pp. 117–148. Springer: Berlin.

12. Cykowski MD, Coon EA, Powell SZ, Jenkins SM, Benarroch EE, Low PA *et al* (2015) Expanding the spectrum of neuronal pathology in multiple system atrophy. *Brain* **138**:2293–2309.

13. Dickson DW. (2012) Parkinson disease and parkinsonism: neuropathology. *Cold Spring Harbor Perspectives in Medicine* **2**: a009258.

14. Dubois B, Slachevsky A, Litvan I, Pillon B (2000) The FAB: a Frontal Assessment Battery at bedside. *Neurology* **55**:1621.

15. Fahn S (2011) Classification of movement disorders. *Mov Disord* **26**:947–957.

16. Folstein MF, Folstein SE, McHugh PR (1975) "Mini-mental state". A practical method for grading the cognitive state of patients for the clinician. *J Psychiatr Res* **12**:189–198.

17. Gellersen HM, Guo CC, O'Callaghan C, Tan RH, Sami S, Hornberger M (2017) Cerebellar atrophy in neurodegeneration-a meta-analysis. *J Neurol Neurosurg Psychiatry* **88**:780–788.

18. Gibb WR, Lees AJ (1988) The relevance of the Lewy body to the pathogenesis of idiopathic Parkinson's disease. *J Neurol Neurosurg Psychiatry* **51**:745–752.

19. Gilman S, Wenning GK, Low PA, Brooks DJ, Mathias CJ, Trojanowski JQ *et al* (2008) Second consensus statement on the diagnosis of multiple system atrophy. *Neurology* **71**:670–676.

20. Gundersen HJ, Bagger P, Bendtsen TF, Evans SM, Korbo L, Marcussen N *et al* (1988) The new stereological tools: disector, fractionator, nucleator and point sampled intercepts and their use in pathological research and diagnosis. *APMIS* **96**:857–881.

21. Gundersen HJ, Jensen EB (1987) The efficiency of systematic sampling in stereology and its prediction. *J Microsc* **147**:229–263.

22. Jellinger KA, Seppi K, Wenning GK (2005) Grading of neuropathology in multiple system atrophy: proposal for a novel scale. *Mov Disord* **20**:S29–S36.

23. Jensen EBV, Gundersen HJ (1993) The rotator. *J Microsc* **170**:35–44.

24. Joelving FC, Billeskov R, Christensen JR, West M, Pakkenberg B (2006) Hippocampal neuron and glial cell numbers in Parkinson's disease–a stereological study. *Hippocampus* **16**:826–833.

25. Karlsen AS, Pakkenberg B (2011) Total numbers of neurons and glial cells in cortex and basal ganglia of aged brains with down syndrome - a stereological study. *Cereb Cortex* **21**:2519–2524.

26. Kawai Y, Suenaga M, Takeda A, Ito M, Watanabe H, Tanaka F *et al* (2008) Cognitive impairments in multiple system atrophy: MSA-C vs MSA-P. *Neurology* **70**: 1390–1396.

27. Kim JS, Yang J, Lee DK, Lee JM, Youn J, Cho JW (2015) Cognitive impairment and its structural correlates in the Parkinsonian subtype of multiple system atrophy. *Neurodegener Dis* **15**:294–300.

28. Köllensperger M, Geser F, Seppi K, Stampfer-Kountchev M, Sawires M, Scherfler C *et al* (2008) Red flags for multiple system atrophy. *Mov Disord* **23**:1093–1099.

29. Kume A, Takahashi A, Hashizume Y, Asai J (1991) A histometrical and comparative study on Purkinje cell loss and olivary nucleus cell loss in multiple system atrophy. *J Neurol Sci* **101**:178–186.

30. Lee MJ, Shin JH, Seoung JK, Lee JH, Yoon U, Oh JH *et al* (2016) Cognitive impairments associated with morphological changes in cortical and subcortical structures in multiple system atrophy of the cerebellar type. *Eur J Neurol* **23**:92–100.

31. Lu CF, Wang PS, Lao YL, Wu HM, Soong BW, Wu YT (2014) Medullo-ponto-cerebellar white matter degeneration altered brain network organization and cortical morphology in multiple system atrophy. *Brain Struct and Funct* **219**:947–958.

32. Mattis S (1976) Mental status examination for organic mental syndrome in the elderly patient. In: Geriatric psychiatry: a handbook for psychiatrists and primary care physicians, L Bellak, TB Karasu (eds), pp. 77–121. Grune & Stratton Inc: New York.

33. Messina D, Cerasa A, Condino F, Arabia G, Novellino F, Nicoletti G *et al* (2011) Patterns of brain atrophy in Parkinson's disease, progressive supranuclear palsy and multiple system atrophy. *Parkinsonism Relat Disord* **17**:172–176.

34. Nykjaer CH, Brudek T, Salvesen L, Pakkenberg B (2017) Changes in the cell population in brain white matter in multiple system atrophy. *Mov Disord* **32**:1074–1082.

35. O'Callaghan C, Hornberger M, Balsters JH, Halliday GM, Lewis SJ, Shine JM (2016) Cerebellar atrophy in Parkinson's disease and its implication for network connectivity. *Brain* **139**:845–855.

36. Ozawa T, Paviour D, Quinn NP, Josephs KA, Sangha H, Kilford L *et al* (2004) The spectrum of pathological involvement of the striatonigral and olivopontocerebellar systems in multiple system atrophy: clinicopathological correlations. *Brain* **127**:2657–2671.

37. Pakkenberg B, Møller A, Gundersen HJ, Mouritzen Dam A, Pakkenberg H (1991) The absolute number of nerve cells in substantia nigra in normal subjects and in patients with Parkinson's disease estimated with an unbiased stereological method. *J Neurol Neurosurg Psychiatry* **54**:30–33.

38. Paviour DC, Price SL, Jahanshahi M, Lees AJ, Fox NC (2006) Regional brain volumes distinguish PSP, MSA-P, and PD: MRI-based clinico-radiological correlations. *Mov Disord* **21**:989–996.

39. Paviour DC, Price SL, Jahanshahi M, Lees AJ, Fox NC (2006) Longitudinal MRI in progressive supranuclear palsy and multiple system atrophy: rates and regions of atrophy. *Brain* **129**:1040–1049.

40. Pedersen KM, Marner L, Pakkenberg H, Pakkenberg B (2005) No global loss of neocortical neurons in Parkinson's disease: a quantitative stereological study. *Mov Disord* **20**:164–171.

41. Pfaffl MW (2001) A new mathematical model for relative quantification in real-time RT-PCR. *Nucleic Acids Res* **29**:e45.

42. Rydbirk R, Elfving B, Andersen MD, Langbøl MA, Folke J, Winge K *et al* (2017) Cytokine profiling in the prefrontal cortex of Parkinson's Disease and Multiple System Atrophy patients. *Neurobiol Dis* **106**:269–278.

43. Rydbirk R, Folke J, Winge K, Aznar S, Pakkenberg B, Brudek T (2016) Assessment of brain reference genes for RT-qPCR studies in neurodegenerative diseases. *Sci Rep* **6**:37116.

44. Salvesen L, Ullerup BH, Sunay FB, Brudek T, Løkkegaard A, Aganader TK *et al* (2015) Changes in total cell numbers of the basal ganglia in patients with multiple system atrophy - a stereological study. *Neurobiol Dis* **74**:104–113.

45. Salvesen L, Winge K, Brudek T, Agander TK, Løkkegaard A, Pakkenberg B (2015) Neocortical neuronal loss in patients with multiple system atrophy: a stereological study. *Cereb Cortex* **27**:400–410.

46. Seidel K, Bouzrou M, Heidemann N, Krüger R, Schöls L, den Dunnen WFA *et al* (2017) Involvement of the cerebellum in Parkinson disease and dementia with Lewy bodies. *Ann Neurol* **81**:898–903.

47. Stokholm J, Vogel A, Johannsen P, Waldemar G (2009) Validation of the Danish Addenbrooke's Cognitive Examination as a screening test in a memory clinic. *Dement Geriatr Cogn Disord* **27**:361–365.

48. Trojanowski J q, Revesz T, Neuropathology Working Group on MSA (2007) Proposed neuropathological criteria for the post mortem diagnosis of multiple system atrophy. *Neuropathol Appl Neurobiol* **33**:615–620.

49. Wenning GK, Krismer F, Poewe W (2011) New insights into atypical parkinsonism. *Curr Opin Neurol* **24**:331–338.

50. Wenning GK, Tison F, Elliott L, Quinn NP, Daniel SE (1996) Olivopontocerebellar pathology in multiple system atrophy. *Mov Disord* **11**:157–162.

51. Witter L, Rudolph S, Pressler RT, Lahlaf SI, Regehr WG (2016) Purkinje cell collaterals enable output signals from the cerebellar cortex to feed back to Purkinje cells and interneurons. *Neuron* **91**:312–319.

52. Wu T, Hallett M (2013) The cerebellum in Parkinson's disease. *Brain* **136**:696–709.

53. Zeng LL, Xie L, Shen H, Luo Z, Fang P, Hou Y *et al* (2017) Differentiating patients with Parkinson's disease from normal controls using gray matter in the cerebellum. *Cerebellum* **16**:151–157.